FRONTIERS OF PHYSICS

RESEARCH ARTICLE
Volume 20 / Issue 4 / 042203 / 2025

Edge solitons in non-Hermitian photonic lattices with type-II Dirac cones

Shuang Shen[1], Milivoj R. Belić[2], Yiqi Zhang[1,†], Yongdong Li[1], Tao Wang[3], Zhen-Nan Tian[4], Qi-Dai Chen[4]

1 Key Laboratory for Physical Electronics and Devices, Ministry of Education, School of Electronic Science and Engineering, Xi'an Jiaotong University, Xi'an 710049, China
2 College of Science and Engineering, Hamad Bin Khalifa University, 23874 Doha, Qatar
3 Grace Laser, Beijing 101318, China
4 State Key Laboratory of Integrated Optoelectronics, College of Electronic Science and Engineering, Jilin University, Changchun 130012, China
Corresponding author. E-mail: †zhangyiqi@xjtu.edu.cn
Received February 15, 2025; accepted March 6, 2025

ABSTRACT

An edge soliton is a localized bound state that arises from the balance between diffraction broadening and nonlinearity-induced self-focusing. It typically resides either at the edge or at the domain wall of a lattice system. To the best of our knowledge, most reported edge solitons have been observed in conservative Hermitian systems; whether stable edge solitons can exist in non-Hermitian systems remains an open question. In this work, we utilize a photonic lattice that naturally exhibits type-II Dirac cones and introduce a domain wall by carefully configuring gains and losses at the three sites within each unit cell. Surprisingly, edge states localized at the domain wall can exhibit entirely real propagation constants. Building on these edge states, we demonstrate the existence of edge solitons that can propagate stably over distances significantly exceeding those in the experimental settings adopted in this study. Although these solitons eventually couple with the bulk states and ultimately collapse, they exhibit remarkable resilience. Our findings establish that a domain wall supporting loss-resistant edge solitons, which can also evade the skin effect, is achievable in non-Hermitian systems. This discovery holds promising potential for the development of compact functional optical devices.

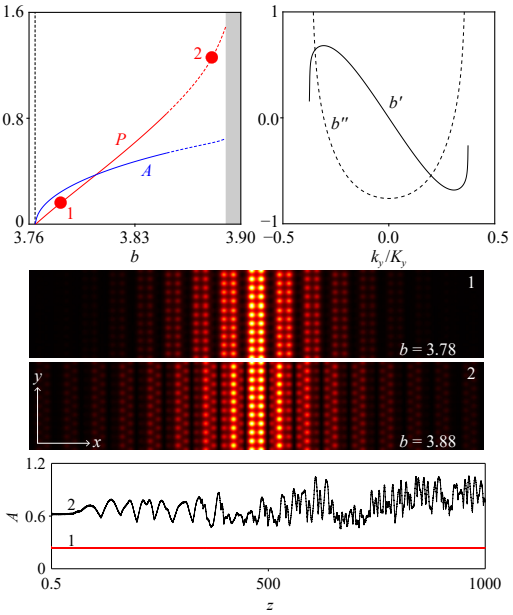

Keywords type-II Dirac cones, non-Hermitian optics, edge solitons

1 Introduction

Non-Hermitian systems, which exchange energy with the environment, present attractive opportunities for investigation, as compared to conservative systems. In 1998, the so-called parity–time ($\mathcal{PT}$) symmetry was proposed, which allowed non-Hermitian systems to possess entirely real eigenvalue spectra, thereby opening up the theoretical study of these systems [1]. One of the most promising advances associated with the $\mathcal{PT}$ symmetry is the optical $\mathcal{PT}$ symmetry [2], because complex potentials corres-

*Special Topic: Topological Dynamics in Ultracold Atoms and Optics (Eds.: Vladimir V. Konotop, Yongyao Li & Boris Malomed).

Higher Education Press

https://doi.org/10.15302/frontphys.2025.042203

ponding to gain/loss regions in photonic materials are relatively easy to realize. The first steps in optical PT symmetry were taken as early as 2008 [3, 4], and band-gap solitons were predicted from the very beginning.

In the following years, the optical $\mathcal{PT}$ symmetry attracted researchers from all over the world, and a wealth of promising results was reported (see review papers [5–11] and references therein). Furthermore, incorporating nonlinearity into non-Hermitian optical systems can lead to the discovery of more intriguing and complex phenomena, such as solitons [4, 12, 13], non-reciprocal light propagation [14], and lasers [15, 16]. Moreover, it has been demonstrated that the $\mathcal{PT}$ symmetry can enhance the influence of nonlinearity on optical materials [17, 18].

In photonic lattices with Dirac cones (named Dirac photonic lattices) the non-Hermitian mechanism will result in the appearance of exceptional rings at the places where Dirac cones are located [19–25]. Unlike type-I Dirac cones [26], whose Fermi surfaces are points, the Fermi surface of a type-II Dirac cone consists of a pair of crossing lines [27–32]. The discovery of photonic lattices that naturally possess type-II Dirac cones [33] enabled the establishment of type-II exceptional rings [34], edge solitons [35–37], and corner states [38] in topological photonics.

However, light modulation in non-Hermitian nonlinear photonic lattices with type-II Dirac cones is still an open problem, since the combination of nonlinearity and non-Hermitivity indeed offers a novel approach to light field modification [39–47]. Especially, the question whether edge solitons can exist in the interplay between type-II exceptional rings and the self-action of nonlinearity is worth pursuing. Concerning spatial solitons in photonic lattices [48–50], there generally exists a power threshold for their establishment, which is quite different from the topological solitons thus far reported [51–53]. Therefore, another relevant question arises, worth answering: are the potentially existing edge solitons in non-Hermitian photonic lattices with type-II Dirac cones thresholdless? These questions are addressed in this paper.

With these tasks at hand, we provide our answers by constructing a domain wall within the photonic lattice with type-II Dirac cones, properly setting the gain and loss to the sites of the lattice. Then, edge states localized at the domain wall will form in the band gap. Since the band gap does not exist in the whole Brillouin zone, the edge states will connect with the type-II exceptional rings. Starting from the linear edge states, the nonlinear edge states will be explored, which are stable in a wide range of the propagation constant. Due to balance between diffraction and nonlinearity, edge solitons will form by superimposing the envelope function onto the linear edge state. These edge solitons can maintain their profiles during propagation over a long distance, far beyond the typical experimental sample lengths. That is, they are protected from losses and the skin effect [54]. To further understand their dynamics, we investigate how the stable propagation distance of these bright edge solitons depends on the gain/loss coefficient. Our analysis reveals a delicate interplay between the nonlinearity and the non-Hermitian mechanism.

2 Results and discussion

2.1 Lattices, band structures, and linear edge states

The dynamics of beam propagation in an imprinted shallow photonic lattice is governed by the nonlinear Schrödinger-like equation, which describes the propagation of the light beam in response to both the lattice potential and nonlinear effects:

$$\mathrm{i}\frac{\partial\psi}{\partial z} = -\frac{1}{2}\nabla^2\psi - \mathcal{R}(x,y)\psi - |\psi|^2\psi. \tag{1}$$

Here, ψ is the complex amplitude of the beam, x and y are the transverse coordinates normalized to some characteristic transverse length r_0, and $\nabla^2 = \partial_x^2 + \partial_y^2$ is the transverse Laplacian. Furthermore, z is the direction of propagation normalized to the diffraction length kr_0^2, where $k = 2\pi n_0/\lambda$ is the light wavenumber (n_0 is the refractive index of the material, and λ the wavelength). The term $\mathcal{R}(x,y)$ describes the photonic lattice; it is a complex function, consisting of two parts, the real and imaginary parts, $\mathcal{R}(x,y) = \mathcal{R}_{\mathrm{re}}(x,y) + \mathrm{i}\mathcal{R}_{\mathrm{im}}(x,y)$. Thus, $\mathcal{R}_{\mathrm{re}}(x,y)$ stands for the refractive index modulation, while $\mathcal{R}_{\mathrm{im}}(x,y)$ indicates gains/losses of the lattice waveguide. Together, they can be described by the Gaussian functions:

$$\mathcal{R}(x,y) = \sum_{m,n}(p_{\mathrm{re}} \pm \mathrm{i}p_{\mathrm{im}})\exp\left[-\frac{(\boldsymbol{r}-\boldsymbol{r}_{m,n})^2}{a^2}\right], \tag{2}$$

where $\boldsymbol{r}_{m,n} = (x_{m,n}, y_{m,n})$ are the coordinates of the lattice and a determines the width of the waveguide. Further, p_{re} is the depth of the waveguide and p_{im} is the gain/loss index of the waveguide. They satisfy the relation:

$$p_{\mathrm{re}} + \mathrm{i}p_{\mathrm{im}} = \frac{k^2 r_0^2}{n_0}(\delta n_{\mathrm{re}} + \mathrm{i}\delta n_{\mathrm{im}}),$$

where $\delta n_{\mathrm{re}} + \mathrm{i}\delta n_{\mathrm{im}}$ represents the complex refractive index change.

For a waveguide made from AlGaAs material, the parameters mentioned are as follows: $n_0 \approx 3.39$, $r_0 = 10$ μm, $\lambda = 1550$ nm, and $a = 0.5$ (5 μm). The refractive index modulation depth is $\delta n_{\mathrm{re}} \sim 1.8\times10^{-3}$ for $p_{\mathrm{re}} = 10$, and the linear gain/loss coefficient is given by $2p_{\mathrm{im}}/(kr_0^2) \sim 0.0728\ \mathrm{cm}^{-1}$ for $p_{\mathrm{im}} = 0.05$. Very recently, it was reported that non-Hermitian waveguide arrays can

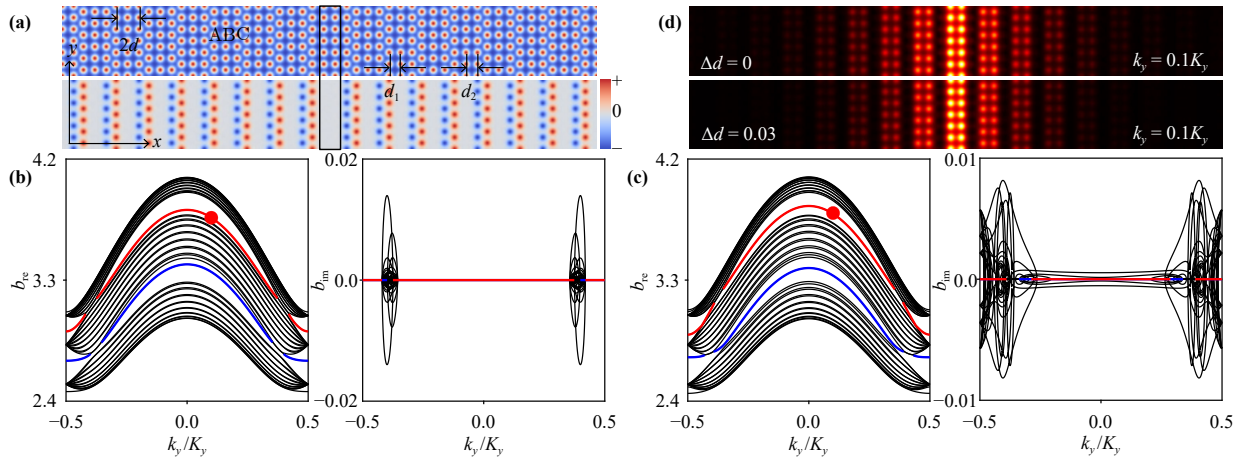

Fig. 1 **(a)** Real (upper panel) and imaginary (lower panel) part of the lattice with a domain wall indicated by the black rectangle. Gains and losses are only exerted on sites A and C, while site B is conserved. The separation between sites A and B in one unit cell is d_1, and that between sites B and C is d_2. The difference between d_1 and d_2 is $\Delta d = d_2 - d_1$. The distance between A and C is $2d$, and is fixed. **(b)** Real (left panel) and imaginary (right panel) parts of the band structure with $\Delta d = 0$. Red and blue lines are the edge modes, while black lines are the bulk states. **(c)** Setup is as in (b) but with $\Delta d = 0.03$. **(d)** Edge states at $k_y = 0.1K_y$, corresponding to the red dots in (b) and (c), presented around the wall. Other parameters: $p_{\text{im}} = 0.05$, $d = 1.6$. Panels in (a, d) are shown in the window $-37.5 \le x \le 37.5$ and $-3d \le y \le 3d$.

be fabricated in Tm-doped BGG glasses by using the femto-second laser direct writing technique [55], which is crucial in topological photonics [56–65].

The unit cell of lattices with type-II Dirac cones contains three lattice sites A, B and C, as seen in Fig. 1. Gain and loss are applied to sites A and C, while site B remains conserved. We define the separation between sites A and B as d_1, and the separation between sites B and C as d_2. The difference between d_1 and d_2 is $\Delta d = d_2 - d_1$. The first row of Fig. 1(a) shows the real part of the lattice structure, when $\Delta d = 0$, while the second row displays the imaginary part. The orange and blue colors represent the amplifying and lossy waveguides, respectively. The lattices are periodic in the y-direction and are constrained in the x-direction, such that $\mathcal{R}(x, y) = \mathcal{R}(x, y + d)$. The region enclosed by the black rectangle in Fig. 1(a) is the domain wall, which is formed by sites B from both the left and the right lattice. According to the imaginary part of the composited lattice in Fig. 1(a), the domain wall is neither gainy nor lossy, as done in the previous literature [47, 66].

The general solution of Eq. (1) is chosen in the form:

$$\psi(x, y, z) = u(x, y) \exp[\mathrm{i}(k_y y + bz)],$$

where $u(x, y) = u(x, y + d)$ is the periodic Bloch wave function, b is the propagation constant, and $k_y \in [-K_y/2, K_y/2]$ is the Bloch momentum in the first Brillouin zone, with $K_y = 2\pi/d$. The function $u(x, y)$ tends to 0 outside the integration window in x. Substituting this solution into Eq. (1) brings about the following steady-state nonlinear wave equation for u:

$$bu = \frac{1}{2}\left(\frac{\partial^2}{\partial x^2} + \frac{\partial^2}{\partial y^2} + 2\mathrm{i}k_y\frac{\partial}{\partial y} - k_y^2\right)u + (\mathcal{R} + |u|^2)u. \tag{3}$$

The band structure of this photonic lattice is obtained by neglecting the nonlinear term in Eq. (3) and using the plane-wave expansion method to solve the remaining linear eigenvalue problem. The results are shown in Figs. 1(b) and (c). From the real part of the band structure in Fig. 1(b), one finds there are two edge states, as highlighted by the red and blue curves, with the bulk states indicated by the black curves. Note that the type-II Dirac cones are replaced by slope-flat regions, which are between the two separated red/blue curves. These flat regions represent type-II exceptional rings [34].

The imaginary part of the band structure in Fig. 1(b) shows that the eigenvalues of the edge states indicated by the red and blue curves are completely real (that is, the imaginary part is 0). Therefore, the edge states are expected to maintain their profiles during propagation in this non-Hermitian lattice. It is worth noting that only the states in the region where the type-II exceptional rings are located are not conserved. In Fig. 1(b), the band structure corresponds to the case $\Delta d = 0$.

In fact, one can also distort the lattice by making $\Delta d \neq 0$, which may help the generation of valley Hall edge states [37]. In Fig. 1(c), we display the band structure corresponding to $\Delta d = 0.03$. One finds that the edge states indicated by the red and blue curves are better localized than the states in Fig. 1(b). The difference can be well illustrated from the edge states in Fig. 1(d), which are chosen from the red curves in Figs. 1(b) and (c), and highlighted by red dots. One also finds that

only the edge states in Fig. 1(c) are Hermitian, while all other states are non-Hermitian. Note also that even though the energy of the edge state is mainly distributed on the domain wall, a portion of energy still penetrates into the bulk, which is non-Hermitian, and that portion of light beam may be affected by the gain/loss. As it will be shown later, the edge soliton is to some extent immune to the gain/loss and exhibits the skin effect avoidance property.

Numerical simulations demonstrate that one cannot distort the lattice too much (even $\Delta d = 0.05$ would be too much), or the edge solitons that will be discussed later will couple with the bulk states, which are amplified during propagation. In the following, we will focus on the cases with $\Delta d = 0$, which do not interfere with the valley Hall effect [35, 67–74]. The quantity Δd can be regarded as a switch for the topological phase transition of the lattice system, and as such represents an additional "degree of freedom" for the manipulation of edge states.

2.2 Nonlinear edge states

Starting from the linear edge state, one can obtain the corresponding nonlinear edge states by applying Newton's iterative method to solve Eq. (3). The family of nonlinear states versus the propagation constant b is presented in Fig. 2(a), corresponding to the red point in Fig. 1(b), for which $k_y = 0.1K_y$. In the figure, the red curve is the power $P = \iint |\psi|^2 \mathrm{d}x\mathrm{d}y$, the blue curve is the peak amplitude $A = \max\{|\psi|\}$, the gray region represents the bulk band, and the black dashed line shows the location of the linear edge state with $b = 3.764$. It is evident that the power shows an almost linear relationship with the propagation constant, while the dependence of the peak amplitude on the propagation constant is close to a parabolic shape along the b axis. Clearly, if the power of the nonlinear edge state decreases to zero, the power curve as well as the peak amplitude curve will cross with the vertical dashed line, which indicates that the nonlinear edge state reduces to its linear counterpart, and also demonstrates that the nonlinear edge state bifurcates from its linear counterpart.

In Fig. 2(b), we show the amplitude modulus of the nonlinear edge state, which corresponds to the red points 1 and 2 in Fig. 2(a). Apparently, most of energy is focused on the domain wall, with some amount penetrating into the bulk. If the propagation constant is getting far from the linear edge state, its localization is becoming worse and worse. In Fig. 2(b), the nonlinear state numbered 1 is better localized than the state numbered 2.

To examine the stability of the nonlinear edge state, we add a small perturbation (up to 10% of the amplitude) to it and then perform a long-distance propagation ($z \sim 5000$) of the perturbed edge state. If it can maintain its profile during such a propagation, we assume that

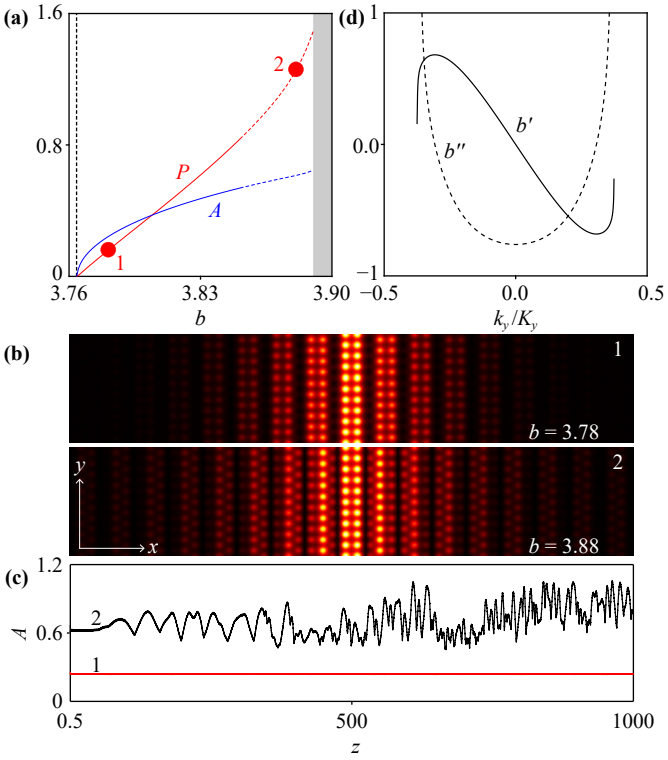

Fig. 2 Nonlinear edge state family bifurcating from the linear edge state. **(a)** The peak amplitude $A = \max\{|\psi|\}$ (blue curve) and the power $P = \iint |\psi|^2 \mathrm{d}x\mathrm{d}y$ (red curve) versus b. The solid and dashed curves represent stable and unstable edge modes. The vertical black dashed line represents the position of the linear edge state, and the gray region represents the bulk band. **(b)** Edge states corresponding to the dots in (a). Parameters are $\Delta d = 0$, $k_y = 0.1K_y$, and $p_{\mathrm{im}} = 0.05$. Panels in (b) are shown in the window $-37.5 \le x \le 37.5$ and $-5d \le y \le 5d$. **(c)** Peak amplitude of the edge state during propagation. Red and black curves correspond to points 1 and 2 in (a). **(d)** First-order b' (solid curve) and second-order b'' (dashed curve) derivatives of the red edge state in Fig. 1(b).

the edge state is stable; otherwise, it is unstable. The stability findings are presented in Fig. 2(a) by the solid (stable) and dashed (unstable) curves. The peak amplitude of the perturbed edge state recorded during propagation that corresponds to the numbered dots in Fig. 2(a), is shown in Fig. 2(c).

The nonlinear edge state indicated by dot 1 is stable, and the recorded peak amplitude indicated by the red line in Fig. 2(c) does not change during propagation. On the other hand, the peak amplitude of the edge state indicated by dot 2 exhibits irregular oscillations, as shown by the black line in Fig. 2(c), which means that the corresponding state is unstable. However, it is worthwhile pointing out that the nonlinear edge state remains stable within a large power and propagation constant range, according to the solid curves in Fig. 2(a).

2.3 Edge solitons

Even though there are stable edge states in this non-Hermitian system, it is still not clear whether edge solitons can be supported or not. The first-order $b' = \mathrm{d}b/\mathrm{d}k_y$ (solid curve) and the second-order $b'' = \mathrm{d}^2b/\mathrm{d}k_y^2$ derivative (dashed curve) of the edge state from Fig. 1(a), that are shown in Fig. 2(d), indicate that the bright edge solitons possibly exist, since $b'' < 0$ in a wide range of b. Note that we do not consider the regions around the boundary of the first Brillouin zone, since the states there tend to be more unstable. Even though there are regions with $b'' > 0$, the corresponding higher-order derivatives would be quite large and the self-trapping from the nonlinearity would not help much the formation of dark edge solitons. Hence, we exclusively use bright edge solitons to describe edge solitons in this paper.

To construct an edge soliton, we adopt the superposition method, and superimpose a soliton envelope onto the linear edge soliton [75–77]. Thus, we assume that the edge soliton can be obtained as a superposition:

$$\psi = \int_{-K_y/2}^{K_y/2} \mathcal{A}(\kappa, z) u(x, y, k+\kappa) \mathrm{e}^{\mathrm{i}bz + \mathrm{i}(k+\kappa)y} \mathrm{d}\kappa,$$

where κ represents the momentum deviation from the momentum k, with the amplitude $\mathcal{A}(\kappa, z)$ defining the envelope. By applying a Taylor series expansion around κ for $u(x, y, k+\kappa)$, one obtains

$$\psi = \mathrm{e}^{\mathrm{i}bz + \mathrm{i}ky} \sum_{n=0,\infty} \frac{(-\mathrm{i})^n}{n!} \frac{\partial^n u(x, y, k)}{\partial k^n} \frac{\partial^n \mathcal{A}(x, z)}{\partial x^n}, \tag{4}$$

where $\mathcal{A}(y, z) = \int_{-K_y/2}^{K_y/2} \mathcal{A}(\kappa, z) \mathrm{e}^{\mathrm{i}\kappa y} \mathrm{d}\kappa$ represents the envelope function of the nonlinear modes. By selecting a gauge such that $\langle u(x, y, k), \partial_k u(x, y, k) \rangle = 0$, the system preserves the $U(1)$ rotation of eigenvector phases, which justifies the assumption that $n = 0$ in Eq. (4). According to the method of Ref. [75], the slowly-varying envelope equation is obtained in the form:

$$\mathrm{i}\frac{\partial \mathcal{A}}{\partial z} = \frac{b''}{2} \frac{\partial^2 \mathcal{A}}{\partial Y^2} - \chi |\mathcal{A}|^2 \mathcal{A}, \tag{5}$$

where $\chi = \int_{-\infty}^{+\infty} \mathrm{d}x \int_0^Y |\phi|^4 \mathrm{d}y$ and $Y = y + b't$. The analytic bright soliton solution of Eq. (3) is thus

$$\mathcal{A} = \sqrt{2\frac{b_{\mathrm{nl}}}{\chi}} \mathrm{sech}\left(Y \sqrt{-2\frac{b_{\mathrm{nl}}}{b''}} \right) \exp(-\mathrm{i}b_{\mathrm{nl}} z), \tag{6}$$

where b_{nl} is the phase shift induced by non-linearity, which should be small for stable solitons.

We construct a representative edge soliton by selecting an edge state at $k_y = 0.15K_y$ from the red line of Fig. 1(b), superimposed with the envelope for $b_{\mathrm{nl}} = 0.005$. In Fig. 3(a), the peak amplitude A of the edge soliton during propagation according to Eq. (1) is displayed, as

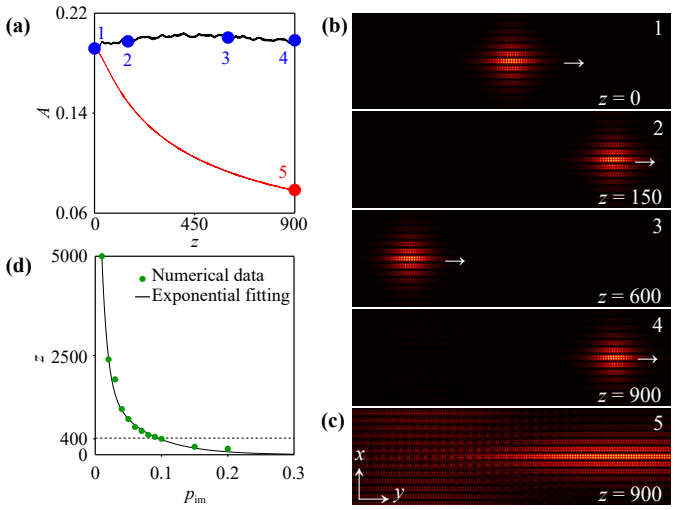

Fig. 3 **(a)** Peak amplitude of the edge soliton during propagation in the non-Hermitian lattice waveguide array with $p_{\mathrm{im}} = 0.05$. Black and red curves are for the linear and nonlinear states. **(b)** Field modulus profiles of the moving edge soliton corresponding to dots 1–4 in (a). The arrow indicates the direction of motion. **(c)** Field modulus profile of the beam corresponding to dot 5 in (a). **(d)** Stable propagation distance of the edge soliton versus p_{im}. Other parameters: $\Delta d = 0$, $k_y = 0.15K_y$, $b_{\mathrm{nl}} = 0.005$, $\chi = 0.094$. Panels in (a, b) are shown in the window $-30 \le x \le 30$ and $-100 \le y \le 100$.

indicated by the black curve. We find that the peak amplitude shows neither amplification nor damping during propagation, even when the distance reaches $z = 900$. We admit that this distance cannot be further continuously extended (it will become corrupted and finally couple with the bulk states). However, the distance of $z = 900$ (corresponding to the experimental distance of ~ 1.2 m) is still far beyond realistic sample lengths. That is, the edge soliton is still a feasible possibility in potential applications. The field modulus profile of edge solitons at selected propagation distances (corresponding to the points 1–4 in Fig. 3(a) are shown in Fig. 3(b). It is evident that soliton propagates in the positive direction along the y-axis, due to $b'' = -0.622$, without radiating into the bulk. Due to the limited computational window, when the beam reaches the right end of the window, it will emerge from the left end of the window, to continue propagating, as shown in Fig. 3(b). If the nonlinearity in Eq. (1) is lifted during propagation, the peak amplitude will decay rapidly, as indicated by the red curve in Fig. 3(a). The profile at $z = 900$ is shown in Fig. 3(c) [corresponding to the point 5 in Fig. 3(a)], where the beam spreads quickly and effectively couples with the bulk states, which are not conservative and exhibit increased radiation during propagation. Even the edge soliton will excite the nonconservative bulk states, if it propagates for a long enough distance. These results demonstrate that the

formation of edge solitons is intrinsically linked to the balance between nonlinearity and diffraction effects.

The stable propagation distance of an edge soliton in this non-Hermitian system strongly depends on the strength of the imaginary part of the potential in Eq. (1). Figure 3(d) shows the dependence of the stabilized propagation distance of the edge soliton with p_{im}, in which the green dots are numerical simulations and the black curve is the corresponding exponential fitting. As p_{im} increases, the stabilized distance decreases approximately exponentially. It can be seen that the stabilized propagation distance is still around $z = 400$ when p_{im} increases to about 0.1, which is around 0.5 m in real units. If one looks at the band structure with even a larger p_{im} (not shown here), e.g., $p_{\mathrm{im}} = 0.3$, one will find that there exists no explicit band gap for the edge state, which for a large enough p_{im} will always couple with the bulk states. Overall, the edge solitons are unstable, but can maintain their profiles unchanged over long applicative distances.

It is worth mentioning that we still refer to the localized states here as edge solitons, even though they are ultimately unstable, because they are indeed resulted from the balance between the diffraction broadening and the nonlinear self-focusing over long real distances. The balance can be illustrated by a direct comparison between the linear propagation in Fig. 3(c) and the nonlinear propagation in Fig. 3(b).

3 Conclusion

Summarizing, we have demonstrated edge solitons in non-Hermitian photonic lattices featuring type-II Dirac cones. These edge solitons are loss-resistant and do not suffer skin effect over a long propagation distance. Although the stability range strongly depends on the gain/loss coefficient, the stable propagation distances are much longer than the typical experimental sample lengths. The results presented not only provide a new platform for deeper understanding of the interplay between non-Hermiticity and nonlinearity, but also possess considerable applicative potential for possible fabrication of on-chip functional optical devices.

Declarations The authors declare that they have no competing interests and there are no conflicts.

Acknowledgements This work was supported by the Natural Science Basic Research Program of Shaanxi Province, China (No. 2024JC-JCQN-06) and the National Natural Science Foundation of China (No. 12474337).

References

1. C. M. Bender and S. Boettcher, Real spectra in non-Hermitian Hamiltonians having PT symmetry, *Phys. Rev. Lett.* 80(24), 5243 (1998)
2. J. Cham, Top 10 physics discoveries of the last 10 years, *Nat. Phys.* 11(10), 799 (2015)
3. K. G. Makris, R. El-Ganainy, D. N. Christodoulides, and Z. H. Musslimani, Beam dynamics in PT symmetric optical lattices, *Phys. Rev. Lett.* 100(10), 103904 (2008)
4. Z. H. Musslimani, K. G. Makris, R. El-Ganainy, and D. N. Christodoulides, Optical solitons in PT periodic potentials, *Phys. Rev. Lett.* 100(3), 030402 (2008)
5. V. V. Konotop, J. Yang, and D. A. Zezyulin, Non-linear waves in PT-symmetric systems, *Rev. Mod. Phys.* 88(3), 035002 (2016)
6. S. Longhi, Parity–time symmetry meets photonics: A new twist in non-Hermitian optics, *Europhys. Lett.* 120(6), 64001 (2017)
7. R. El-Ganainy, K. G. Makris, M. Khajavikhan, Z. H. Musslimani, S. Rotter, and D. N. Christodoulides, Non-Hermitian physics and PT symmetry, *Nat. Phys.* 14(1), 11 (2018)
8. M. A. Miri and A. Alù, Exceptional points in optics and photonics, *Science* 363(6422), eaar7709 (2019)
9. Y. Ashida, Z. Gong, and M. Ueda, Non-Hermitian physics, *Adv. Phys.* 69(3), 249 (2020)
10. S. K. Gupta, Y. Zou, X. Y. Zhu, M. H. Lu, L. J. Zhang, X. P. Liu, and Y. F. Chen, Parity–time symmetry in non-Hermitian complex optical media, *Adv. Mater.* 32(27), 1903639 (2020)
11. C. Wang, Z. Fu, W. Mao, J. Qie, A. D. Stone, and L. Yang, Non-Hermitian optics and photonics: From classical to quantum, *Adv. Opt. Photonics* 15(2), 442 (2023)
12. S. Nixon, L. Ge, and J. Yang, Stability analysis for solitons in PT-symmetric optical lattices, *Phys. Rev. A* 85(2), 023822 (2012)
13. K. Komagata, A. Tusnin, J. Riemensberger, M. Churaev, H. Guo, A. Tikan, and T. J. Kippenberg, Dissipative Kerr solitons in a photonic dimer on both sides of exceptional point, *Commun. Phys.* 4(1), 159 (2021)
14. H. Ramezani, T. Kottos, R. El-Ganainy, and D. N. Christodoulides, Unidirectional nonlinear PT-symmetric optical structures, *Phys. Rev. A* 82(4), 043803 (2010)
15. B. Peng, Ş. K. Özdemir, S. Rotter, H. Yilmaz, M. Liertzer, F. Monifi, C. M. Bender, F. Nori, and L. Yang, Loss-induced suppression and revival of lasing, *Science* 346(6207), 328 (2014)
16. S. Shen, Y. V. Kartashov, Y. Li, M. Cao, and Y. Zhang, π mode lasing in the non-Hermitian Floquet topological system, *APL Photonics* 9(8), 086113 (2024)
17. X. Y. Lü, H. Jing, J. Y. Ma, and Y. Wu, PT–symmetry-breaking chaos in optomechanics, *Phys. Rev. Lett.* 114(25), 253601 (2015)
18. J. Zhang, B. Peng, Ş. K. Özdemir, Y. Liu, H. Jing, X. y. Lü, Y. Liu, L. Yang, and F. Nori, Giant nonlinearity via breaking parity–time symmetry: A route to low-threshold phonon diodes, *Phys. Rev. B* 92(11), 115407 (2015)
19. B. Zhen, C. W. Hsu, Y. Igarashi, L. Lu, I. Kaminer, A. Pick, S. L. Chua, J. D. Joannopoulos, and M. Soljačić, Spawning rings of exceptional points out of Dirac cones, *Nature* 525(7569), 354 (2015)

20. M. Parto, Y. G. N. Liu, B. Bahari, M. Khajavikhan, and D. N. Christodoulides, Non-Hermitian and topological photonics: Optics at an exceptional point, *Nanophotonics* 10(1), 403 (2020)
21. H. Wang, X. Zhang, J. Hua, D. Lei, M. Lu, and Y. Chen, Topological physics of non-Hermitian optics and photonics: A review, *J. Opt.* 23(12), 123001 (2021)
22. A. Li, H. Wei, M. Cotrufo, W. Chen, S. Mann, X. Ni, B. Xu, J. Chen, J. Wang, S. Fan, C. W. Qiu, A. Alù, and L. Chen, Exceptional points and non-Hermitian photonics at the nanoscale, *Nat. Nanotechnol.* 18(7), 706 (2023)
23. H. Nasari, G. G. Pyrialakos, D. N. Christodoulides, and M. Khajavikhan, Non-Hermitian topological photonics, *Opt. Mater. Express* 13(4), 870 (2023)
24. Q. Wang and Y. D. Chong, Non-Hermitian photonic lattices: Tutorial, *J. Opt. Soc. Am. B* 40(6), 1443 (2023)
25. Q. Yan, B. Zhao, R. Zhou, R. Ma, Q. Lyu, S. Chu, X. Hu, and Q. Gong, Advances and applications on non-Hermitian topological photonics, *Nanophoton.* 12, 2247 (2023)
26. Y. Wang, F. Zhang, M. Zeng, H. Sun, Z. Hao, Y. Cai, H. Rong, C. Zhang, C. Liu, X. Ma, L. Wang, S. Guo, J. Lin, Q. Liu, C. Liu, and C. Chen, Intrinsic magnetic topological materials, *Front. Phys. (Beijing)* 18(2), 21304 (2023)
27. G. G. Pyrialakos, N. S. Nye, N. V. Kantartzis, and D. N. Christodoulides, Emergence of type-II Dirac points in graphyne-like photonic lattices, *Phys. Rev. Lett.* 119(11), 113901 (2017)
28. G. G. Pyrialakos, N. Schmitt, N. S. Nye, M. Heinrich, N. V. Kantartzis, A. Szameit, and D. N. Christodoulides, Symmetry-controlled edge states in the type-II phase of Dirac photonic lattices, *Nat. Commun.* 11(1), 2074 (2020)
29. C. Hu, Z. Li, R. Tong, X. Wu, Z. Xia, L. Wang, S. Li, Y. Huang, S. Wang, B. Hou, C. T. Chan, and W. Wen, Type-II Dirac photons at metasurfaces, *Phys. Rev. Lett.* 121(2), 024301 (2018)
30. C. R. Mann, T. J. Sturges, G. Weick, W. L. Barnes, and E. Mariani, Manipulating type-I and type-II Dirac polaritons in cavity-embedded honeycomb metasurfaces, *Nat. Commun.* 9(1), 2194 (2018)
31. X. Wu, X. Li, R. Y. Zhang, X. Xiang, J. Tian, Y. Huang, S. Wang, B. Hou, C. T. Chan, and W. Wen, Deterministic scheme for two-dimensional type-II Dirac points and experimental realization in acoustics, *Phys. Rev. Lett.* 124(7), 075501 (2020)
32. M. Milićević, G. Montambaux, T. Ozawa, O. Jamadi, B. Real, I. Sagnes, A. Lemaître, L. Le Gratiet, A. Harouri, J. Bloch, and A. Amo, Type-III and tilted Dirac cones emerging from flat bands in photonic orbital graphene, *Phys. Rev. X* 9(3), 031010 (2019)
33. K. C. Jin, H. Zhong, Y. D. Li, F. W. Ye, Y. P. Zhang, F. L. Li, C. L. Liu, and Y. Q. Zhang, Parametric type-II Dirac photonic lattices, *Adv. Quantum Technol.* 3(7), 2000015 (2020)
34. Q. Tang, M. R. Belić, H. Zhong, M. Cao, Y. Li, and Y. Zhang, *PT*-symmetric photonic lattices with type-II Dirac cones, *Opt. Lett.* 49(15), 4110 (2024)
35. H. Zhong, S. Xia, Y. Zhang, Y. Li, D. Song, C. Liu, and Z. Chen, Nonlinear topological valley Hall edge states arising from type-II Dirac cones, *Adv. Photonics* 3(5), 056001 (2021)
36. Y. Tian, Y. Zhang, Y. Li, and M. R. Belić, Vector valley Hall edge solitons in the photonic lattice with type-II Dirac cones, *Front. Phys. (Beijing)* 17(5), 53503 (2022)
37. Y. Tian, Y. Wang, M. R. Belić, Y. Zhang, Y. Li, and F. Ye, Vector valley Hall edge solitons in distorted type-II Dirac photonic lattices, *Opt. Express* 31(13), 20812 (2023)
38. S. Feng, H. Zhong, M. R. Belić, D. Mihalache, Y. Li, and Y. Zhang, Bound-in-continuum-like corner states in the type-II Dirac photonic lattice, *Chaos Solitons Fractals* 181, 114719 (2024)
39. R. Driben and B. A. Malomed, Stability of solitons in parity–time-symmetric couplers, *Opt. Lett.* 36(22), 4323 (2011)
40. D. Leykam, V. V. Konotop, and A. S. Desyatnikov, Discrete vortex solitons and parity time symmetry, *Opt. Lett.* 38(3), 371 (2013)
41. M. Ögren, F. K. Abdullaev, and V. V. Konotop, Solitons in a *PT*-symmetric $\chi^{(2)}$ coupler, *Opt. Lett.* 42(20), 4079 (2017)
42. Z. Chen, J. Huang, J. Chai, X. Zhang, Y. Li, and B. A. Malomed, Discrete solitons in self-defocusing systems with *PT*-symmetric defects, *Phys. Rev. A* 91(5), 053821 (2015)
43. Z. Chen, J. Liu, S. Fu, Y. Li, and B. A. Malomed, Discrete solitons and vortices on two-dimensional lattices of *PT*-symmetric couplers, *Opt. Express* 22(24), 29679 (2014)
44. M. Wimmer, A. Regensburger, M. A. Miri, C. Bersch, D. N. Christodoulides, and U. Peschel, Observation of optical solitons in *PT*-symmetric lattices, *Nat. Commun.* 6(1), 7782 (2015)
45. S. V. Suchkov, A. A. Sukhorukov, J. Huang, S. V. Dmitriev, C. Lee, and Y. S. Kivshar, Nonlinear switching and solitons in *PT*-symmetric photonic systems, *Laser Photonics Rev.* 10(2), 177 (2016)
46. A. L. M. Muniz, M. Wimmer, A. Bisianov, U. Peschel, R. Morandotti, P. S. Jung, and D. N. Christodoulides, 2D solitons in *PT*-symmetric photonic lattices, *Phys. Rev. Lett.* 123(25), 253903 (2019)
47. S. Xia, D. Kaltsas, D. Song, I. Komis, J. Xu, A. Szameit, H. Buljan, K. G. Makris, and Z. Chen, Nonlinear tuning of *PT* symmetry and non-Hermitian topological states, *Science* 372(6537), 72 (2021)
48. F. Lederer, G. I. Stegeman, D. N. Christodoulides, G. Assanto, M. Segev, and Y. Silberberg, Discrete solitons in optics, *Phys. Rep.* 463(1–3), 1 (2008)
49. Y. V. Kartashov, B. A. Malomed, and L. Torner, Solitons in nonlinear lattices, *Rev. Mod. Phys.* 83(1), 247 (2011)
50. B. A. Malomed and D. Mihalache, Nonlinear waves in optical and matter-wave media: A topical survey of recent theoretical and experimental results, *Rom. J. Phys.* 64, 106 (2019)
51. D. Mihalache, Localized structures in optical and matter-wave media: A selection of recent studies, *Rom. Rep. Phys.* 73, 403 (2021)

52. Y. V. Kartashov, S. K. Ivanov, Y. Q. Zhang, S. A. Zhuravitskii, N. N. Skryabin, I. V. Dyakonov, A. A. Kalinkin, S. P. Kulik, V. O. Kompanets, S. V. Chekalin, and V. N. Zadkov, Experiments with non-linear topological edge states in static and dynamically modulated Su–Schrieffer–Heeger arrays, *Phys. Uspekhi* 67(11), 1095 (2024)
53. W. Zhang, X. Chen, Y. V. Kartashov, V. V. Konotop, and F. Ye, Coupling of edge states and topological Bragg solitons, *Phys. Rev. Lett.* 123(25), 254103 (2019)
54. R. Lin, T. Tai, L. Li, and C. H. Lee, Topological non-Hermitian skin effect, *Front. Phys. (Beijing)* 18(5), 53605 (2023)
55. A. Dupont, S. Leonov, T. Guérineau, Y. Messaddeq, J. Lapointe, and R. Vallée, Lasing in a femtosecond-laser-written single-scan waveguide fabricated in Tm-doped BGG glass, *Opt. Lett.* 50(2), 666 (2025)
56. M. C. Rechtsman, J. M. Zeuner, Y. Plotnik, Y. Lumer, D. Podolsky, F. Dreisow, S. Nolte, M. Segev, and A. Szameit, Photonic Floquet topological insulators, *Nature* 496(7444), 196 (2013)
57. M. S. Kirsch, Y. Zhang, M. Kremer, L. J. Maczewsky, S. K. Ivanov, Y. V. Kartashov, L. Torner, D. Bauer, A. Szameit, and M. Heinrich, Nonlinear second-order photonic topological insulators, *Nat. Phys.* 17(9), 995 (2021)
58. X. L. Zhang, F. Yu, Z. G. Chen, Z. N. Tian, Q. D. Chen, H. B. Sun, and G. Ma, Non-Abelian braiding on photonic chips, *Nat. Photonics* 16(5), 390 (2022)
59. Y. K. Sun, X. L. Zhang, F. Yu, Z. N. Tian, Q. D. Chen, and H. B. Sun, Non-Abelian Thouless pumping in photonic waveguides, *Nat. Phys.* 18(9), 1080 (2022)
60. L. C. Wang, Y. Chen, M. Gong, F. Yu, Q. D. Chen, Z. N. Tian, X. F. Ren, and H. B. Sun, Edge state, localization length, and critical exponent from survival probability in topological waveguides, *Phys. Rev. Lett.* 129(17), 173601 (2022)
61. Y. V. Kartashov, A. A. Arkhipova, S. A. Zhuravitskii, N. N. Skryabin, I. V. Dyakonov, A. A. Kalinkin, S. P. Kulik, V. O. Kompanets, S. V. Chekalin, L. Torner, and V. N. Zadkov, Observation of edge solitons in topological trimer arrays, *Phys. Rev. Lett.* 128(9), 093901 (2022)
62. B. Ren, A. A. Arkhipova, Y. Zhang, Y. V. Kartashov, H. Wang, S. A. Zhuravitskii, N. N. Skryabin, I. V. Dyakonov, A. A. Kalinkin, S. P. Kulik, V. O. Kompanets, S. V. Chekalin, and V. N. Zadkov, Observation of nonlinear disclination states, *Light Sci. Appl.* 12(1), 194 (2023)
63. A. A. Arkhipova, Y. Zhang, Y. V. Kartashov, S. A. Zhuravitskii, N. N. Skryabin, I. V. Dyakonov, A. A. Kalinkin, S. P. Kulik, V. O. Kompanets, S. V. Chekalin, and V. N. Zadkov, Observation of π solitons in oscillating waveguide arrays, *Sci. Bull. (Beijing)* 68(18), 2017 (2023)
64. H. Zhong, V. O. Kompanets, Y. Zhang, Y. V. Kartashov, M. Cao, Y. Li, S. A. Zhuravitskii, N. N. Skryabin, I. V. Dyakonov, A. A. Kalinkin, S. P. Kulik, S. V. Chekalin, and V. N. Zadkov, Observation of nonlinear fractal higher order topological insulator, *Light Sci. Appl.* 13(1), 264 (2024)
65. W. Yan, B. Zhang, and F. Chen, Photonic topological insulators in femtosecond laser direct-written waveguides, *npj Nanophoton.* 1, 40 (2024)
66. S. Weimann, M. Kremer, Y. Plotnik, Y. Lumer, S. Nolte, K. G. Makris, M. Segev, M. C. Rechtsman, and A. Szameit, Topologically protected bound states in photonic parity–time-symmetric crystals, *Nat. Mater.* 16(4), 433 (2017)
67. Q. Tang, B. Ren, V. O. Kompanets, Y. V. Kartashov, Y. Li, and Y. Zhang, Valley Hall edge solitons in a photonic graphene, *Opt. Express* 29(24), 39755 (2021)
68. B. Ren, H. Wang, V. O. Kompanets, Y. V. Kartashov, Y. Li, and Y. Zhang, Dark topological valley Hall edge solitons, *Nanophotonics* 10(13), 3559 (2021)
69. Q. Tang, Y. Zhang, Y. V. Kartashov, Y. Li, and V. V. Konotop, Vector valley Hall edge solitons in superhoneycomb lattices, *Chaos Solitons Fractals* 161, 112364 (2022)
70. Q. Tang, B. Ren, M. R. Belić, Y. Zhang, and Y. Li, Valley Hall edge solitons in the kagome photonic lattice, *Rom. Rep. Phys.* 74, 504 (2022)
71. H. Xue, Y. Yang, and B. Zhang, Topological valley photonics: Physics and device applications, *Adv. Photon. Res.* 2(8), 2100013 (2021)
72. G. J. Tang, X. T. He, F. L. Shi, J. W. Liu, X. D. Chen, and J. W. Dong, Topological photonic crystals: Physics, designs, and applications, *Laser Photonics Rev.* 16(4), 2100300 (2022)
73. X. Zhu, Y. Chen, Z. Liu, Y. Han, and Z. Qiao, Valley-polarized quantum anomalous Hall effect in van der Waals heterostructures based on monolayer Jacutingaite family materials, *Front. Phys. (Beijing)* 18(2), 23302 (2023)
74. S. Pan, Z. Li, and Y. Han, Electric-field-tunable topological phases in valley-polarized quantum anomalous Hall systems with inequivalent exchange fields, *Front. Phys. (Beijing)* 20(1), 14207 (2025)
75. S. K. Ivanov, Y. V. Kartashov, A. Szameit, L. Torner, and V. V. Konotop, Vector topological edge solitons in Floquet insulators, *ACS Photonics* 7(3), 735 (2020)
76. S. K. Ivanov, Y. V. Kartashov, L. J. Maczewsky, A. Szameit, and V. V. Konotop, Edge solitons in Lieb topological Floquet insulator, *Opt. Lett.* 45(6), 1459 (2020)
77. S. K. Ivanov, Y. V. Kartashov, L. J. Maczewsky, A. Szameit, and V. V. Konotop, Bragg solitons in topological Floquet insulators, *Opt. Lett.* 45(8), 2271 (2020)